



HAL
open science

Analysis of the relationship between backscattered P-band radar signals and soil roughness

Mehrez Zribi, M. Sahnoun, N. Baghdadi, Thuy Le Toan, A. Ben Hamida

► **To cite this version:**

Mehrez Zribi, M. Sahnoun, N. Baghdadi, Thuy Le Toan, A. Ben Hamida. Analysis of the relationship between backscattered P-band radar signals and soil roughness. *Remote Sensing of Environment*, 2016, 186, pp.13-21. hal-01394292

HAL Id: hal-01394292

<https://hal.science/hal-01394292>

Submitted on 9 Nov 2016

HAL is a multi-disciplinary open access archive for the deposit and dissemination of scientific research documents, whether they are published or not. The documents may come from teaching and research institutions in France or abroad, or from public or private research centers.

L'archive ouverte pluridisciplinaire **HAL**, est destinée au dépôt et à la diffusion de documents scientifiques de niveau recherche, publiés ou non, émanant des établissements d'enseignement et de recherche français ou étrangers, des laboratoires publics ou privés.

1 **Analysis of the relationship between backscattered P-band radar signals** 2 **and soil roughness**

3 **M. Zribi¹, M. Sahnoun^{1,2}, N. Baghdadi³, T. Le Toan¹, A. Ben Hamida²**

4
5 ¹CESBIO (CNRS/UPS/IRD/CNES), 18 av. Edouard Belin, bpi 2801, 31401 Toulouse cedex9,
6 France.

7 ²ENIS/Université de Sfax, Route Soukra Km 3.5, Sfax, Tunisia.

8 ³IRSTEA, UMR TETIS, 500 rue François Breton, 34093 Montpellier cedex 5, France.

9 10 11 **Abstract**

12
13 In this paper, the potential use of P-band radar signals for the estimation of soil roughness
14 parameters is analyzed. The numerical moment method backscattering model is used to study
15 the sensitivity to soil roughness parameters of backscattered P-band signals. Two roughness
16 scales related to terrain microtopography and low frequency roughness structures are
17 considered. In the case of microtopography, the rms height is shown to be the dominant
18 influence in the relationship between radar signals and roughness. For low frequency
19 structures, the parameter Z_s is strongly correlated with the backscattered signals. An analysis
20 of the behavior of P-band radar signals as a function of multi-scale soil roughness
21 (microtopography and large-scale roughness structures) reveals the complexity of using P-
22 band data for the study of bare surface soil parameters.

23 The Moment method model is then compared with the real data covering a large range of
24 microtopographic roughness values, derived from experimental airborne P-band SAR
25 campaigns made over agricultural fields, at two sites in France. The significant discrepancies
26 observed between measurements and simulations confirm the limitations of an analysis based
27 on microtopographic characterizations only.

28

29 **Keywords: SAR, P-band, bare soil, roughness, moment method**

30

31 **1- Introduction**

32

33 Soil moisture and roughness parameters play a key role in hydrological and climatic studies.

34 In recent years, considerable effort has been devoted to the analysis of the backscattering

35 characteristics of bare soils. Different backscattering models (theoretical (analytical or

36 numerical), semi-empirical and empirical) were developed (Ulaby et al., 1986, Fung et al.,

37 1992, Oh et al., 1992, Dubois et al., 1995, Chen et al., 2003, Zribi et al., 2006, Huang et al.,

38 2010, Huang et al., 2012, Tsang et al., 2012). Recently, several studies have proposed various

39 approaches to the improvement of roughness descriptions (Oh et al., 1998, Davison et al.,

40 2000, Mattia et al., 2001, Zribi et al., 2003, Callens et al., 2006, Baghdadi et al., 2006,

41 Verhoest et al., 2008, Lievens et al., 2009, Zribi et al., 2014a), which are essential to the

42 accurate analysis and interpretation of backscattering behavior and soil moisture estimation.

43 Almost all studies based on the interpretation of radar measurements make use of signals

44 recorded in the L, C and X bands. For these different bands, which are generally derived from

45 satellite or airborne measurements, various algorithms have been developed to estimate

46 roughness and soil moisture for agricultural soils (Rahman et al., 2008, Paloscia et al., 2010,

47 Pierdicca et al., 2010, Zribi et al., 2011, Gerboudj et al., 2011, Gorrab et al., 2015).

48 Roughness is generally described by two parameters: the RMS height (H_{rms}), and the

49 correlation length (l) of the soil, derived from its height correlation function, which is often

50 considered to have a Gaussian or exponential shape. In the case of applications involving

51 agricultural soils, this function is generally assumed to be exponential (Zribi et al., 1997).

52 Fung et al. (1994), Shi et al. (1997) and Zribi et al. (2005) have also proposed different types

53 of analytical correlation function to fit the experimental data. In a context where only a small

54 number of radar configurations was available for the inversion of surface parameters, Zribi
55 and Dechambre (2003) introduced a description based on the parameter $Z_s = Hrms^2/l$. The
56 strength of backscattered radar signals is sensitive to variations in surface roughness,
57 especially in the case of low levels of roughness (rms height approximately <1 cm in the X-
58 band, 1.5 cm in the C-band, and 2 cm in the L-band), (Baghdadi et al., 2006). The results
59 obtained using L, C, and X-band data show that in the case of bare soils, the radar signal (σ^0)
60 has an exponential or logarithmic dependence on soil surface roughness (Baghdadi et al.,
61 2002; Zribi et al., 2003), and increases linearly with the volumetric soil moisture (mv) when
62 the latter lies in the range between approximately 5 and 35 Vol.% (e.g. Aubert et al., 2013). In
63 the last years, different studies have also analyzed effects of low frequency roughness
64 structures, particularly row directional effects (Ulaby et al., 1982, Rakotaoraivony et al., 1996,
65 Davidson et al., 2002, Zribi et al., 2002, Blaes et al., 2008). However, because of large
66 number of unknown surface parameters, they are often neglected in radar signal inversion.
67 Whereas the vast majority of research involving P-band radar measurements has been related
68 to the mapping of forest characteristics, very few studies have investigated the characteristics
69 of these signals over bare soils (Baghdadi et al., 2013). In this context, with the planned 2020
70 launch of the P-band SAR mission BIOMASS, devoted to the study of the biomass of the
71 Earth's forests (Le Toan et al., 2011), there is a call to analyze the potential use of this
72 frequency band for other applications - in particular roughness and moisture estimations for
73 bare or covered soils. In the present study, we therefore discuss the application of P-band
74 measurements to the estimation of these parameters. Our paper is organized in four sections.
75 Section 2 presents our analysis of P-band backscattering behavior over rough soils, computed
76 with the numerical moment method (MM). This section discusses the influence of
77 microtopography and low frequency roughness structures, as well as that of multi-scale
78 roughness surfaces on backscattering simulations. Section 3 presents an intercomparison of

79 results produced by the numerical moment method and real radar data acquired over
80 agricultural fields. Finally, our conclusions are presented in Section 4.

81 **2- Analysis of backscattering behavior over rough soils**

82 The aim of this section is to use exact numerical simulations to analyze the backscattering
83 behavior of P-band radar signals, as a function of roughness. For this analysis, we consider
84 two roughness scales: surface microtopography resulting from soil tillage (clods, etc), and
85 low-frequency scale features that can be produced by small local variations in topography or
86 directional tillage.

87 2-1 Moment method simulations

88 The backscattering computation is based on the numerical resolution of two integral
89 equations, defined as follows:

90 - in air:

$$91 \quad \vec{n} \times \vec{E}^i(\vec{r}) = -\frac{1}{2} \vec{K} + \vec{n} \times \int_c \left[j\omega\mu_0 G_1 \vec{J} - \vec{K} \times \nabla G_1 - \frac{\nabla' \cdot \vec{J}}{j\omega\epsilon_1} \nabla G_1 \right] dl'$$

$$92 \quad \vec{n} \times \vec{H}^i(\vec{r}) = -\frac{1}{2} \vec{J} + \vec{n} \times \int_c \left[j\omega\epsilon_1 G_1 \vec{K} + \vec{J} \times \nabla G_1 - \frac{\nabla' \cdot \vec{K}}{j\omega\mu_0} \nabla G_1 \right] dl' \quad (1)$$

93 - in soil, the corresponding integral equations are:

$$94 \quad 0 = -\frac{1}{2} \vec{K} - \vec{n} \times \int_c \left[j\omega\mu_0 G_2 \vec{J} - \vec{K} \times \nabla G_2 - \frac{\nabla' \cdot \vec{J}}{j\omega\epsilon_2} \nabla G_2 \right] dl'$$

$$95 \quad 0 = -\frac{1}{2} \vec{J} - \vec{n} \times \int_c \left[j\omega\epsilon_0 G_2 \vec{K} + \vec{J} \times \nabla G_2 - \frac{\nabla' \cdot \vec{K}}{j\omega\epsilon_2} \nabla G_2 \right] dl' \quad (2)$$

96 where μ_0 is the permeability of air, ϵ_1 and ϵ_2 are the dielectric constants of air and soil,
97 respectively, and \vec{n} is the unit outward normal to the surface. $\vec{J} = \vec{n} \times \vec{H}$ is the equivalent

98 surface electric current density, and $\vec{J} = -\vec{n} \times \vec{E}$ is the equivalent surface magnetic current
 99 density.

100 The Green functions are defined in cylindrical coordinates, by the zeroth order Hankel
 101 function of the second kind, as:

$$102 \quad G_i = -\frac{j}{4} H_0^{(2)}(k_i |\vec{\rho} - \vec{\rho}'|), i = 1, 2 \quad (3)$$

103 In order to implement these numerical simulations, a large number of surfaces with varying
 104 roughness parameters was generated. For this step, we consider the approach described by
 105 (Fung et al, 1985), in which the following procedure is applied:

106 the surface heights h are written as:

$$107 \quad h(k) = \sum_{i=-M}^{i=M} W(i) X(i+k) \quad (4)$$

108 where $X(i)$ is a Gaussian random variable $N(0,1)$, and $W(i)$ is the weighting function given by
 109 $W(i) = F^{-1}[\sqrt{F[C(i)]}]$, in which $C(i)$ is the correlation function and $F[]$ denotes the Fourier
 110 transform operator. In the numerical simulations, a Fast Fourier Transformation (FFT) is used
 111 to compute the corresponding values of $W(i)$.

112 Following several convergence tests, the profile length was set to approximately 20λ , where
 113 λ is the wavelength corresponding to the radar frequency ($f=0.43$ GHz) used in the
 114 simulations, and the number of profiles was set to 50. For each profile, a small cell size was
 115 selected ($\lambda/100$), thus allowing an accurate analysis to be made of the contributions of
 116 microtopographic structures to the simulated backscattering behavior. Although our results
 117 are shown for the HH polarization only, very similar behaviors were observed in the VV
 118 polarization.

121 2-2 Analysis of the moment method model's sensitivity to soil roughness

122 In order to study the influence of soil roughness (small-scale, low frequency structures) on
123 radar signal backscattering in the P-band, moment method simulations were run in the *HH*
124 and *VV* polarizations, at 20° and 40° incidence angles.

125 The soil surfaces generated using this approach are considered to have an exponential
126 correlation function, of the form $\rho(x) = Hrms^2 \exp\left(-\frac{x}{l}\right)$ for small roughness scales, and

127 $\rho_G(x) = Sg^2 \exp\left(-\frac{x}{Lg}\right)$ for low spatial frequency roughness scales.

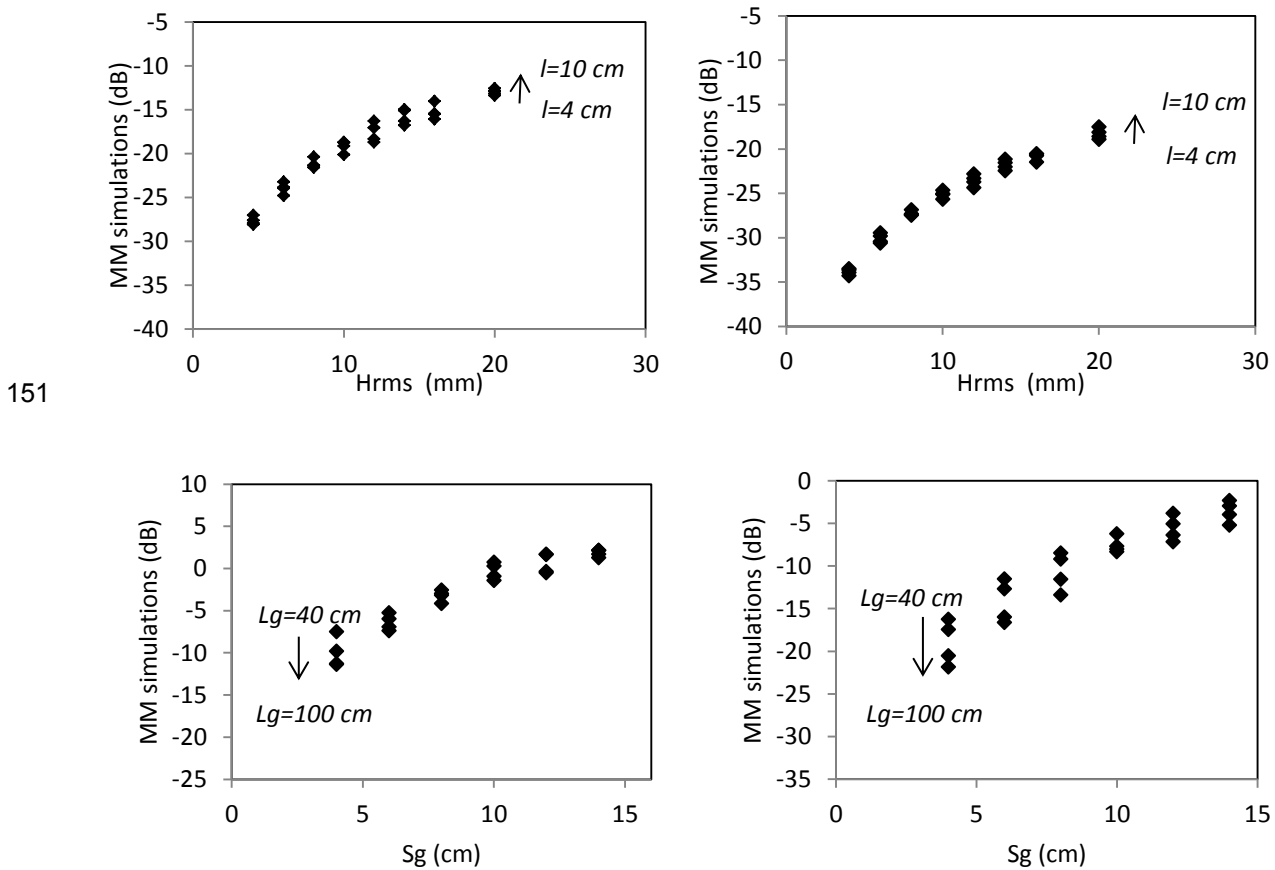
128

129 The dielectric constant is estimated as a function of the volumetric soil moisture and texture,
130 using the empirical model of Pelinsky (Pelinski et al. 1995a, Pelinski et al., 1995b), developed
131 for frequencies in the range between 0.4 and 1.3 GHz. Fig. 1 (a and b) show the simulated
132 backscattering coefficients as a function of rms surface height (*Hrms*), computed in the P-
133 band (0.43 GHz) at 20° and 40° incidence angles. Various surface roughness parameters
134 corresponding to the ranges generally retrieved for agricultural soils were used: *Hrms*
135 between 0.4 and 2 cm; correlation lengths (*l*) between 4 and 10 cm. These simulations show
136 that the backscattered signal is well correlated with *Hrms* (R^2 equal to 0.97 and 0.99, at 20°
137 and 40°, respectively), and that when *Hrms* remains constant only a small increase in
138 backscattered radar signal is produced by variations in correlation length: a difference of
139 approximately 1.0 ~ 1.5 dB is observed between the shortest and longest correlation lengths
140 (4 cm and 10 cm). This increase in signal strength is in contradiction with the decrease
141 observed in the C and X bands, using the same dynamic range for the roughness parameters
142 retrieved (in general) from real agricultural soils (Zribi et al., 2003, Zribi et al., 2014a). This
143 change in behavior between frequency bands is related to variations in the roughness
144 spectrum, as shown in Fig. 2, where this function is plotted (in dB) as a function of wave

145 number (k), using two different correlation lengths (4 and 10 cm), for the case of an

146 exponential correlation function given by:
$$W = \frac{k^4 l^2 H_{rms}^2}{(1 + (2kl \sin \theta)^2)^{1.5}}$$

147 Firstly, it can be seen in Fig. 2 that the difference between the spectral power at these two
 148 correlation lengths undergoes a sign change, when the wave number increases beyond
 149 $\sim 0.16 \text{ cm}^{-1}$. Secondly, with the MM simulations, the correlation length has a relatively minor
 150 influence on the roughness spectrum at low frequencies.

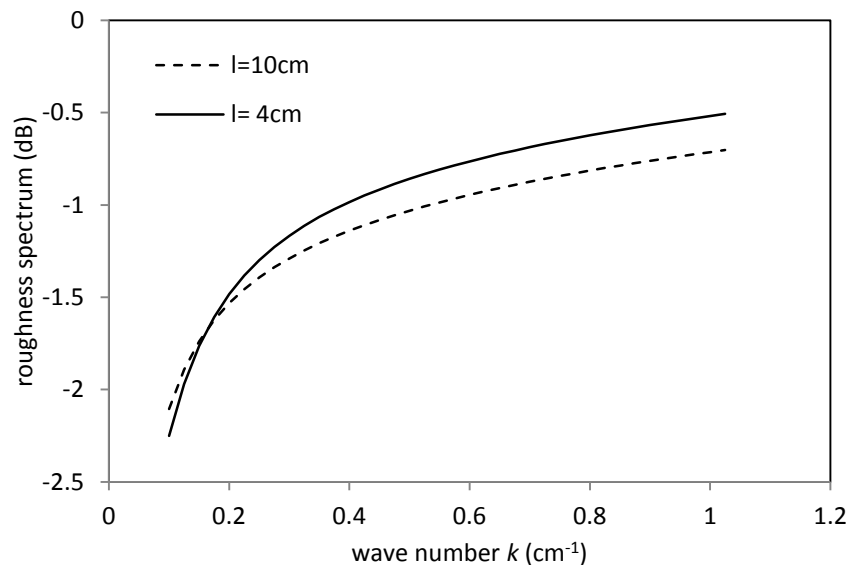


153 Figure 1: Backscattering simulations as a function of surface roughness, corresponding in the
 154 case of (a) and (b) to: microtopography (H_{rms}) with correlation lengths l equal to 4, 6, 8
 155 and 10 cm, and in the case of (c) and (d) to: a low spatial frequency rms height (S_g),
 156 with correlation lengths L_g equal to 40, 60, 80 and 100 cm. All simulations are made in
 157 the HH polarization with a volumetric soil moisture value of 20 Vol.%. The simulations

158 in (a) and (c) are made at a 20° incidence angle, and those of (b) and (d) are made at a
 159 40° incidence angle.

160

161 To a first approximation, the MM simulations thus show that a study of the role of
 162 microtopography roughness can be limited to variations in the parameter Hrms.



163

164 **Figure 2: Exponential roughness spectrum as a function of wave number**

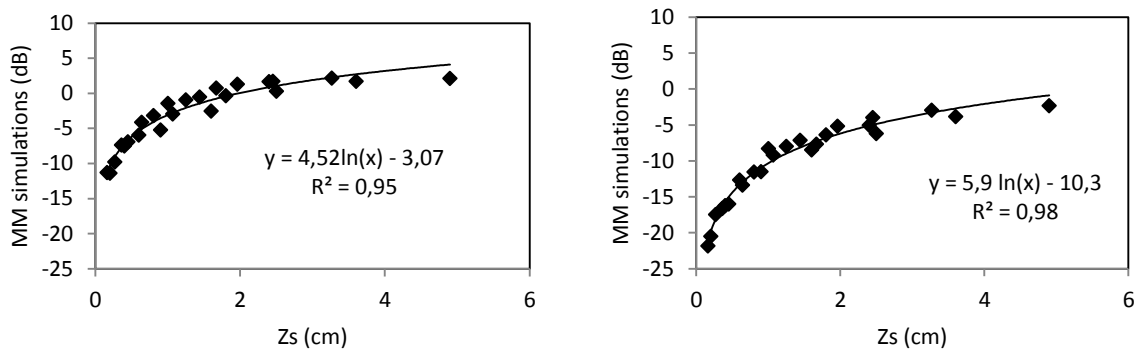
165

166 Fig. 1 (c and d) plots the simulated backscattering MM signals as a function of the rms height
 167 S_g . Several surface parameters were chosen ($S_g = 4$ cm, $S_g = 6$ cm, $S_g = 8$ cm, $S_g = 10$ cm, S_g
 168 $= 12$ cm, $S_g = 14$ cm; $L_g = 40$ cm, $L_g = 60$ cm, $L_g = 80$ cm and $L_g = 100$ cm).

169 For these roughness values, we observe an increase in radar signal strength as a function of
 170 increasing rms height S_g , and a decrease in simulated radar signal as a function of increasing
 171 correlation length L_g .

172 The parameter Z_s , defined by (Zribi et al., 2003) as $Z_s = S_g^2 / L_g$ and tested with C and X
 173 bands data in other studies, is evaluated here. As shown in Fig. 3, the relationship between Z_s
 174 and the simulated radar signals is strongly correlated under all roughness conditions, with R^2

175 equal to 0.95 and 0.98 at angles of incidence equal to 20° and 40°, respectively. We thus
 176 consider that, at this scale it is sufficient to use Z_s alone, to describe the radar signal's
 177 behavior as a function of the soil roughness.



178
 179 **Figure 3:** Backscattering simulations in the HH polarization, as a function of the parameter Z_s
 180 (cm): S_g lies in the range between 4 and 14 cm, L_g between 40 and 100 cm, $mv = 20$ Vol.%
 181 (cm^3/cm^3) a) 20° incidence angle, b) 40° incidence angle.

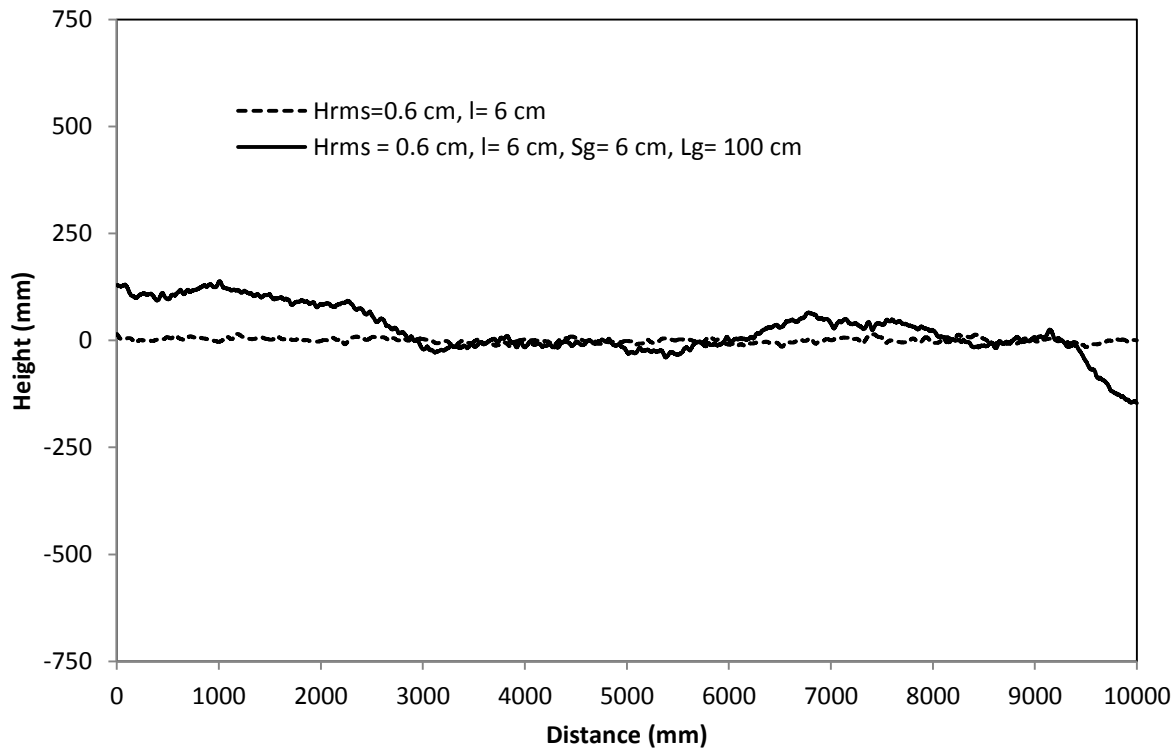
182 2-3 Analysis of the effects of multi-scale roughness in moment method simulations

183 In general, when natural or agricultural soils are observed, two main roughness components
 184 are observed: small-scale roughness corresponding to soil microtopography tillage (cloddy
 185 structures), and large-scale roughness corresponding to local variations in terrain height,
 186 and/or directional effects (Rakotoarivony et al., 1996). For this reason, in the present section
 187 we analyze the radar signal's sensitivity to multi-scale roughness, including the effects of
 188 micro-topography and low frequency roughness structures. We thus consider synthetic soil
 189 profiles respecting the correlation function, with small and low roughness scales:

$$190 \quad \rho(x) = Hrms^2 \exp\left(-\frac{x}{l}\right) + Sg^2 \exp\left(-\frac{x}{Lg}\right) \quad (5)$$

191 Fig. 4 provides two examples of synthetic surface profiles: the first of these has small-scale
 192 roughness parameters only ($Hrms=0.6\text{cm}$, $l=6\text{cm}$), whereas the second is characterized by

193 multi-scale roughness, combining the latter small-scale parameters with the additional effects
 194 of low frequency roughness structures ($S_g=6$ cm, $L_g=100$ cm).

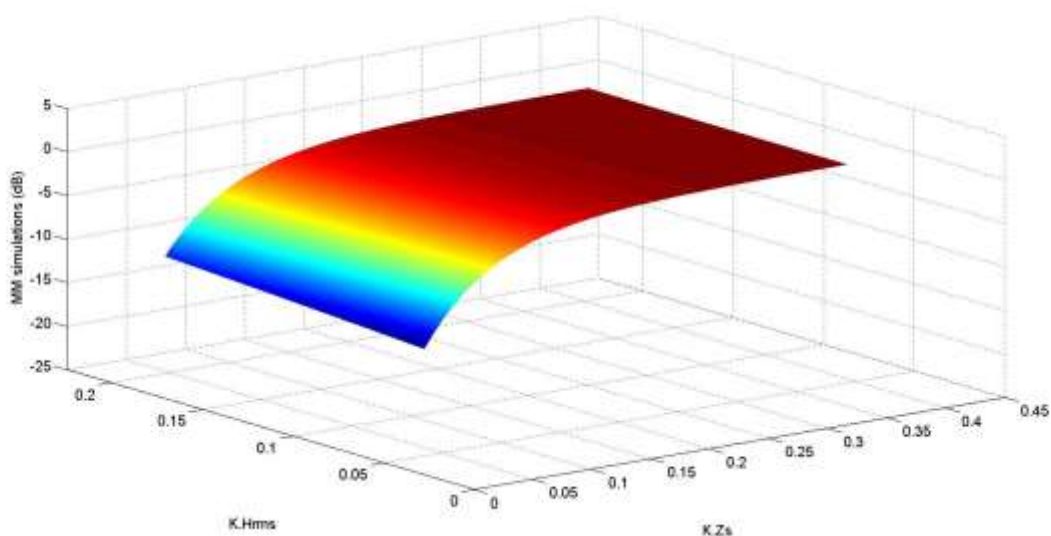


195
 196 **Figure 4:** Synthetically generated surface profiles: micro-topography ($H_{rms}=0.6$ cm, $l=6$ cm)
 197 and multi-scale roughness ($H_{rms}=0.6$ cm, $l=6$ cm, $S_g=6$ cm, $L_g=100$ cm).

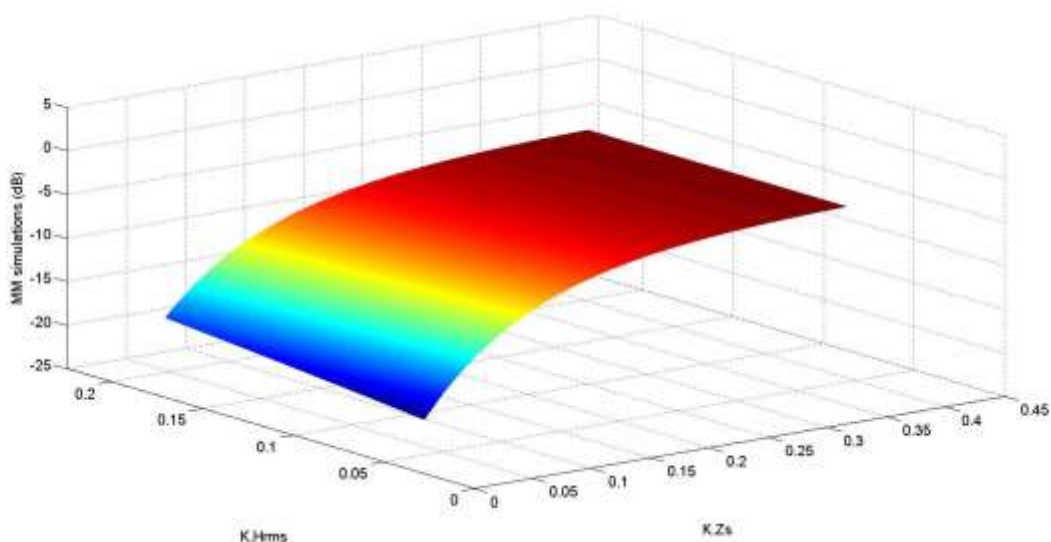
198
 199 Two parameters, H_{rms} describing the terrain's micro-topography, and Z_s describing low
 200 frequency roughness structures, can be used to analyze the behavior of radar signals under
 201 multi-scale roughness conditions.

202 Fig. 5 plots the results of radar signal simulations for these multi-scale surfaces, in the HH
 203 polarization at 20° and 40° incidences, as a function of the two roughness parameters: $k.H_{rms}$
 204 in the range between 0.036 and 0.19; and $k.Z_s$ between 0.015 and 0.45 (corresponding to S_g in
 205 the range between 4 and 14 cm and L_g in the range between 40 and 100 cm). The simulated
 206 backscattering coefficients increase when the values of the two roughness parameters $k.Z_s$ and
 207 $k.H_{rms}$ increase.

208 For a constant value of $k.Zs$, only small variations (less than one decibel) in simulated radar
209 signal are observed due to variations in $k.Hrms$ (micro-topography). As shown in the
210 preceding section, the radar signals with the highest dynamic range are produced by terrain
211 having low frequency structures, with a difference of approximately 12 dB between the
212 extreme values of $k.Zs$. As can be seen in Fig. 6, the MM backscattered signals come close to
213 saturation at high values of $k.Zs$ (>0.2).



214



215

216

217 Figure 5: MM backscattering simulations (in decibels) as a function of the two roughness
 218 parameters ($k.Hrms$, $k.Zs$), at a) 20° incidence angle, b) 40° incidence angle.

219 In the previous discussions we consider a roughness spectrum produced by the sum of two
 220 independent exponential spectra corresponding to the small, and to the low spatial frequency,
 221 roughness scales described above. We thus retrieve two dominant roughness parameters for
 222 the backscattering simulations: $k.Zs$ and $k.Hrms$. From these results, we propose to use the
 223 following roughness spectrum:

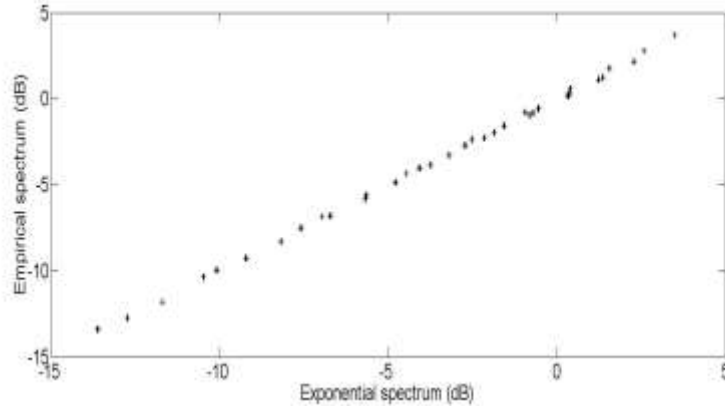
$$224 \quad W(2k \sin \theta) = a_\theta (k.Hrms)^{b_\theta} + c_\theta (k.Zs)^{d_\theta} \quad (6)$$

225 where a_θ , b_θ , c_θ , d_θ are empirical parameters retrieved, as shown in Table 1, by fitting this
 226 relationship to the two constituent exponential roughness spectra (corresponding to small and
 227 low spatial frequency scales).

228 Table 1: Empirical values of the roughness parameters a_θ , b_θ , c_θ and d_θ .

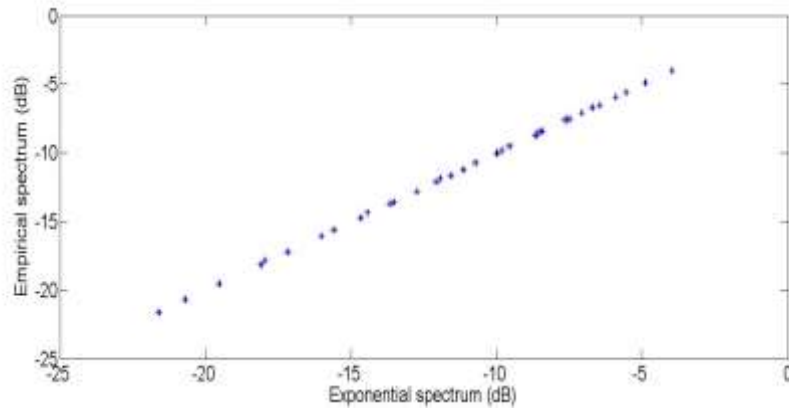
angle	a_θ	b_θ	c_θ	d_θ
20°	5.4	1.73	2.32	1.03
40°	3.6	2.95	0.42	0.98

229
 230 Figure 6 compares the analytical and empirical exponential spectra proposed for all roughness
 231 combinations (more than 1000 different sets of conditions, covering the ranges considered for
 232 $Hrms$, l , Sg and Lg) used in the simulations described above. These are found to be in very
 233 good agreement, with RMS errors equal to 0.12 dB and 0.05 dB at incidence angles equal to
 234 20° and 40° , respectively.



235

236



237

238 Figure 6: Intercomparison between roughness spectrum values retrieved with exponential
 239 spectrum and empirical relationship (6), for all roughness conditions considered for MM
 240 simulations ($Hrms$ ranged between 0.4 cm and 2 cm, l ranged between 4 and 10 cm, Sg
 241 ranged between 4 and 14cm and Lg ranged between 40 and 100 cm), at incidence angle equal
 242 to: a) 20° incidence angle, b) 40° incidence angle.

243

244 From these results, we propose the following empirical relationship to express the
 245 backscattered radar signal as a function of the two variables ($k.Hrms$ and $k.Zs$), for one
 246 polarization and one value of incidence angle:

247
$$\sigma^0 = \alpha_{\theta,p} + \beta_{\theta,p} \left(1 - e^{-\left(\mu_{\theta,p} k.Zs + \gamma_{\theta,p} k.Hrms \right)} \right) \quad (7)$$

248 where σ^0 is expressed in dB, k in cm^{-1} , $Hrms$ in cm and Zs in cm.

249

250 For incidence angles equal to 20° and 40° , the values of α , β , μ and γ are provided in Table 2.

251 The value of α is related to soil moisture effects. In the absence of low scale surface

252 roughness, μ is equal to zero. In the absence of microtopographical soil roughness, γ is equal to

253 zero.

254 Table 2: Values of the empirical model parameters, for incidence angles equal to 20°

255 and 40° , in the HH polarization.

Incidence angle	α	β	μ	γ
20°	-15.8	17.07	1.55	0.099
40°	-23.6	20.21	0.99	0.12

256

257 In Fig. 7 the backscattered signal strength given by the calibrated empirical model (Eq. 6) is

258 compared to that predicted by the MM simulations, at incidence angle equal to 20° and 40°

259 and for the same roughness conditions as those illustrated in Fig. 6. The two models are found

260 to be in very good agreement, with an RMSE equal to 0.7 dB and 0.8 dB, and R^2 equal to 0.98

261 and 0.97, for incidence angle equal to 20° and 40° respectively. This outcome illustrates the

262 usefulness of this empirical relationship, for the prediction of radar backscattering behavior as

263 a function of soil roughness. The empirical model is validated for all of the roughness

264 conditions analyzed by the moment method simulations, in which $k.Hrms$ ranges between

265 0.036 and 0.18, and $k.Zs$ ranges between 0.015 and 0.45.

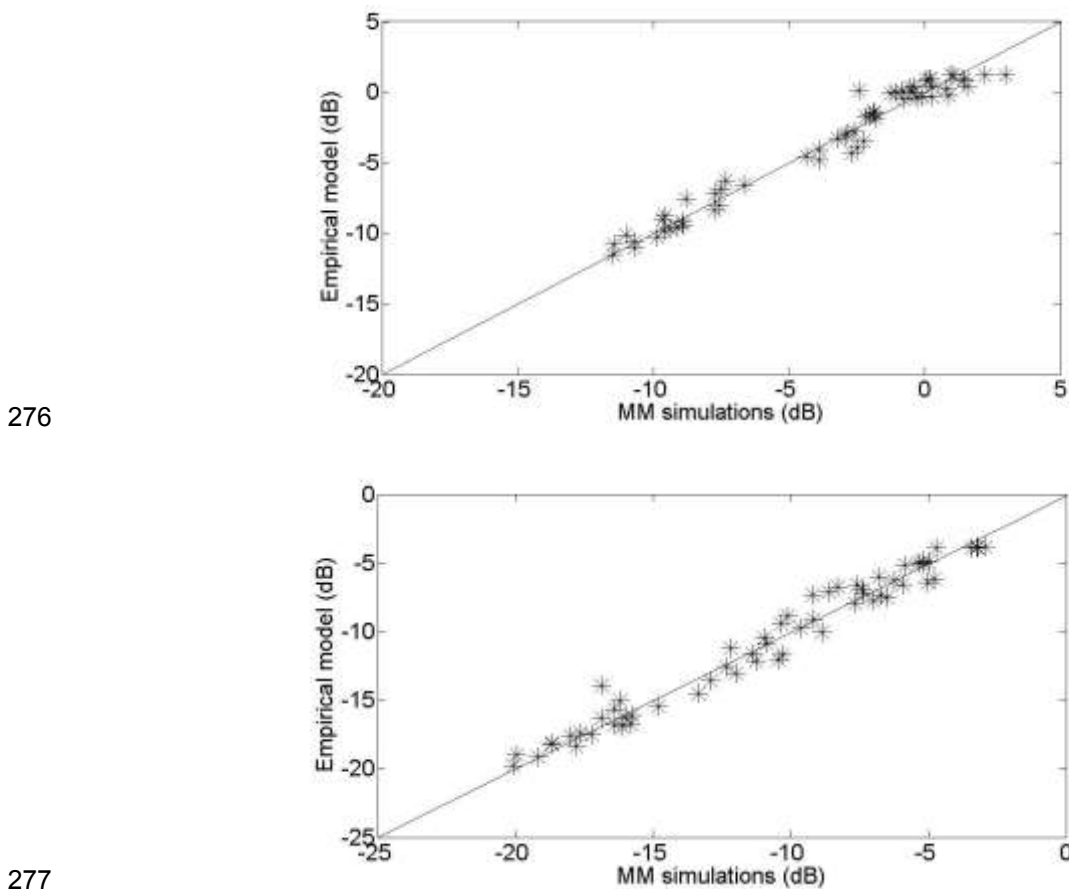
266 The parameter $k.Zs$ clearly dominates the relationship between roughness and radar signal

267 strength. If the latter parameter is used alone in the empirical exponential relationship (i.e. the

268 influence of $k.Hrms$ is ignored in Eq. 6), the RMSE increases to 0.9 dB and 1.2 dB, at

269 incidence angles equal to 20° and 40° , respectively.

270 This analysis, based on the implementation of only two independent parameters ($k.Hrms$ and
271 $k.Zs$), is very well adapted to the use of an inversion approach, which generally makes use of
272 a limited number of radar configuration measurements (often just one or two). For the
273 purposes of direct modeling, an analysis based on the use of all roughness parameters ($Hrms$,
274 l , Sg and Lg) could be useful for a more detailed analysis of the role of roughness and soil
275 surface characteristics.



278 Figure 7: Comparison of radar backscattering predicted by the empirical model defined in
279 equation (6), with the results predicted by MM simulations using the same set of roughness
280 conditions as for the simulations shown in Fig. 5, at incidence angles equal to a) 20°, b) 40°.

281

282 The preceding description reveals the somewhat complex relationship between P-band radar
283 signals and soil roughness: in the absence of an accurate knowledge of the soil's low

284 frequency roughness structures, the backscattering analysis is likely to be affected by
285 significant errors.

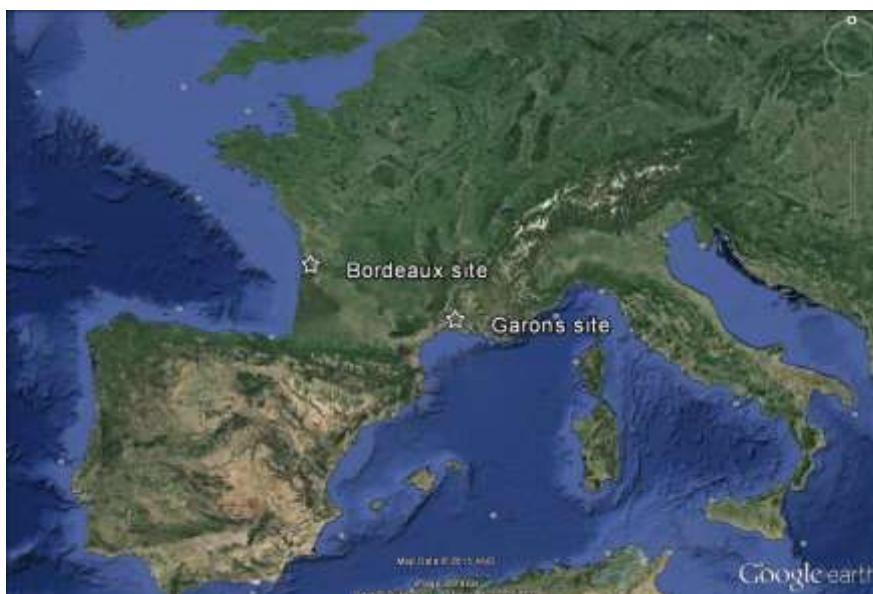
286 **3- Comparison between MM backscattering simulations and experimental P-band data**

287 3-1 Description of the database

288 Our database is comprised of fully polarimetric acquisitions recorded from airborne SAR
289 (Synthetic Aperture Radar) sensors, together with ground measurements, corresponding to
290 several agricultural study sites in France (Fig. 8, Table 3).

291 ***Bordeaux site:*** this site is located in the southwest of France (long. 0°50'W, lat. 45°17'N).
292 The soil is comprised of approximately 19% silt, 29% clay, and 51% sand. On January 21,
293 2004, fully polarimetric P-band radar data (435 MHz) was acquired by the airborne RAMSES
294 SAR, operated by the French Aerospace Research Center (ONERA). The spatial resolution of
295 these SAR images was 2.5 m in range and azimuth.

296 ***Garons site:*** this site is located near to Nîmes in the South of France (long. 04°23'E, lat.
297 43°45'N). The soil is stony, and is comprised of 54% silt, 40% clay, and 6% sand. Fully
298 polarimetric radar data were acquired in the UHF-band (360 MHz, spatial resolution
299 approximately 0.75 m) on October 4th, 2011, using the new multispectral airborne SAR
300 system known as SETHI, operated by the ONERA.



301

302

Figure 8: Location of two study sites in France (Bordeaux and Garons).

303

304 Ground truth measurements of soil moisture and surface roughness were carried out

305 simultaneously with SAR sensor observations of eight reference plots, each of which has a

306 surface area of at least one hectare. Only bare soils or soils with scattered short grass were

307 selected. The soil roughness measurements were made using 1 m long needle profilometers

308 with 2 cm sampling intervals. From ten roughness profiles measured on each reference field,

309 the root mean square (H_{rms}) surface height and correlation length (Table 2) were computed

310 from the mean values of all correlation functions. Gravimetric soil moisture samples were

311 collected from the top 10 cm of soil at random locations in each field, and the volumetric

312 water content at the scale of each field was taken to be the mean of the water content values of

313 the individual samples (10 to 40 measurements per plot). In the case of the ground truth

314 campaign made at the Bordeaux site, the four bare soil plots were very wet, with moisture

315 contents ranging between 26.9 Vol.% and 46.9 Vol.%. However, the Garons site was very

316 dry, with soil moisture contents ranging between 2.8 Vol.% and 4.4 Vol.% (Table 1).

317 The RAMSES and SETHI data were radiometrically calibrated, and their polarimetric

318 parameters were then extracted. Coherency matrices are frequently processed for speckle

319 reduction, using a sliding window to compute the average values of several neighboring
320 pixels.

321 The PolSARPro v4.2.0 software (<http://earth.eo.esa.int/polsarpro/>) was used to process the
322 polarimetric SAR data. The backscattering coefficients in the HH and VV polarizations were
323 averaged using a 15x15 pixel sliding window.

324 **Table 3:** Characteristics of the ground truth measurements. θ : Incidence angle, m_v :
325 Volumetric soil moisture (0-10 cm), $Hrms$: Root mean square surface height, l : Correlation
326 length.

Study site	Plot number	θ ($^\circ$)	m_v (Vol.%)	$Hrms$ (cm)	l (cm)
Bordeaux	Bare soil (B1)	53 $^\circ$	26.9	1.89	4.33
	Bare soil (B2)	47 $^\circ$	46.9	0.88	3.22
	Bare soil (B3)	50 $^\circ$	32.9	1.31	3.95
	Bare soil (B4)	52 $^\circ$	39.4	1.69	4.30
Garons	Bare soil (G1)	43 $^\circ$	4	1.56	4.80
	Bare soil (G2)	45 $^\circ$	4.3	1.40	3.34
	Bare soil (G3)	34 $^\circ$	4.4	0.59	3.27
	Bare soil (G4)	46 $^\circ$	2.8	1.25	3.80

327

328

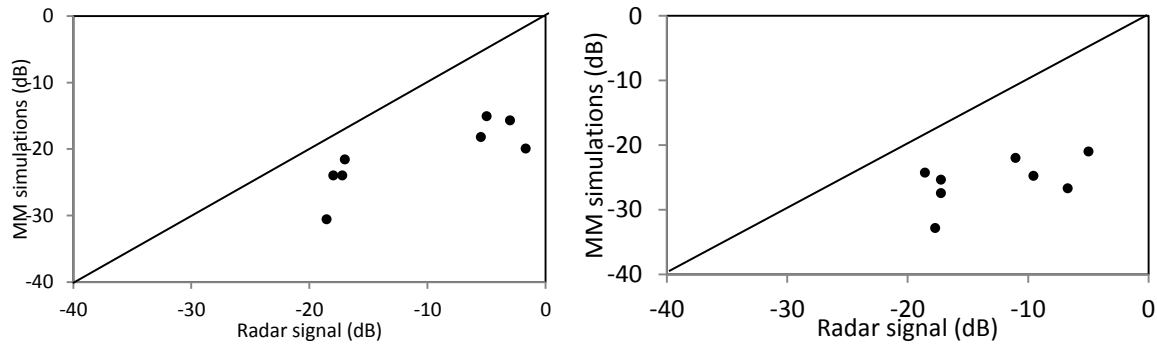
329 3-2 Intercomparison of real data and backscattering model simulations

330 In Fig. 9, the results produced with the MM model are compared with real radar data, for the
331 *HH* and *VV* polarizations, respectively. For each individual test field, ground truth
332 measurements (*Hrms* height, correlation length, soil moisture) were used in the radar
333 backscattering simulations. As can be seen in Fig. 9, considerable discrepancies are found
334 between the measurements and simulations, for both *HH* and *VV* polarizations, with an
335 RMSE equal to 13.4 and 11.2 dB, respectively. These differences cannot be explained by
336 excursions from the validity domain of the (exact) MM model. As shown in the last section,
337 low frequency structures have a dominant effect on backscattering signals. However, the

338 terrain's low frequency roughness structures were not taken into account in our simulations,
339 since they could not be measured with a simple 1 or 2 m pin profiler. This is one possible
340 explanation for the large values of RMSE found with these results.

341 Another possible source of errors in the simulated radar signals is the heterogeneity of the
342 vertical soil moisture profile. This effect has been discussed for the case of higher
343 frequencies, in the L, C and X bands (Le Morvan et al., 2008, Zribi et al., 2014b). In these
344 bands, soil moisture heterogeneity generally has a limited effect on the backscattered radar
345 signals. In the P-band, the penetration depth defined by $\delta = \frac{\lambda\sqrt{\epsilon'}}{2\pi\epsilon''}$ (where $\epsilon = \epsilon' - i\epsilon''$ is the
346 relative dielectric constant) is greater. This effect has been analyzed in (Zribi et al., 2016)
347 through the use of two multi-layer models, the SSA (Small Slope Approximation) and the
348 SPM (Small Perturbation Model), applied to various different simulated moisture profiles.
349 The results show that even relatively extreme conditions, characterized by dry surface soils
350 and wet soils at greater depths, affect the radar signal by not more than 1.5 dB. Two types of
351 extreme conditions were recorded in our database: very wet and very dry conditions ($mv > 27$
352 Vol.% and $mv < 4.5\%$ Vol.%). In both cases, only small heterogeneities are observed in the
353 vertical moisture profiles.

354 Volume scattering is a third possible cause of the aforementioned errors. Our database
355 comprises wet and dry soils, and for both types we found nearly the same discrepancies
356 between the simulations and radar measurements. However, it should be noted that volume
357 scattering is negligible in the case of wet surfaces ($mv > 27$ Vol.%), as a consequence of the
358 radar signal's reduced penetration depth (Ulaby et al., 1986).



359

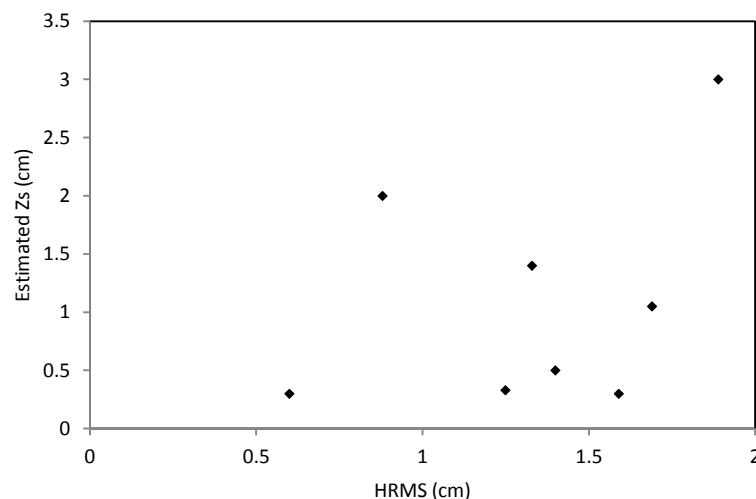
360 Figure 9: Simulated MM radar signals as a function of measured radar signals over
 361 agricultural fields, a) HH pol (b) VV pol

362 From this analysis, we assume that low frequency structures probably play the most
 363 significant role, in terms of induced errors, when they are not accounted for in the
 364 simulations.

365 3-3 Application of the proposed empirical inversion model

366 From the conclusions of the previous section, and in the absence of ground truth
 367 measurements allowing the real value of low spatial frequency roughness to be determined,
 368 the proposed empirical model described in Eq. (7) is used here, to retrieve the roughness
 369 parameter Z_s corresponding to eight test fields.

370 When H_{rms} (microtopography) and the incidence angle are known, Z_s can be retrieved from
 371 Eq. (7). Figure 10 plots the retrieved values of Z_s as a function of H_{rms} , for the eight test
 372 fields. Z_s can be seen to range between 0.3 and 3 cm, i.e. to the range of values considered in
 373 our simulations of agricultural soils. Four of the fields were selected at the Garons site, and
 374 have quite small values of Z_s , between approximately 0.3 and 0.5 cm. This indicates a small
 375 level of low frequency variations, and is confirmed by the very flat characteristics of the
 376 studied site. Although ground truth measurements would be needed to verify this result, it
 377 confirms the robustness of the analyses described in the previous sections, based on numerical
 378 and empirical simulations.



379

380 Figure 10: Estimated values of Z_s , plotted as a function of the in situ values of H_{rms}

381

measured on eight test fields

382 **3-4 Numerical example of errors produced by ground measurement inadequacies**

383 In this section, we use numerical simulations to show that the backscattering model is affected

384 by increasingly strong errors, when the size of the ground measurement profile is decreased,

385 in the presence of low frequency terrain structures. Ground measurements are generally based

386 on the use of a pin profiler of limited length (one to two meters). The height correlation

387 function is then estimated using the mean values of the roughness parameters derived from n 388 profiles. In the following, we present the results of radar signal simulations ($f=0.43$ GHz)

389 computed using different mean roughness values. The latter are derived from a numerically

390 generated 150 m profile, which is subsequently divided into n profiles, having lengths ranging391 from 1 m ($n=150$) to 15 meters ($n=10$). Fig. 11 shows the simulated MM radar signal strength392 (using mean roughness values as input) as a function of the lengths of the n profiles. An initial

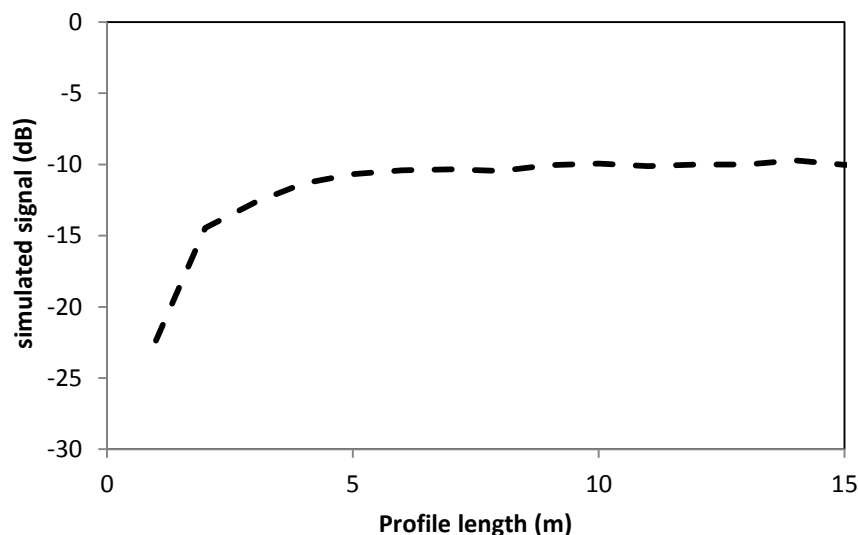
393 increase in the value of the backscattering coefficient can be observed when the length of the

394 profiles is increased, and convergence is nearly achieved when the length of the profiles

395 reaches approximately 6 m. This result clearly illustrates the risk of generating large errors,

396 when the profiles are not sufficiently long with respect to the low frequency structure of the

397 terrain (Baghdadi et al, 2000). This threshold for the profile lengths may not be completely
398 constant, and can depend on the nature of the low frequency structures present in the observed
399 terrain.



400
401 **Figure 11:** Variations in simulated radar signal as a function of the length of the soil profiles,
402 including the effects of multiscale roughness ($Hrms=0.6$ cm, $l=6$ cm, $Sg=6$ cm, $Lg=100$ cm)

403

404 4- Conclusions

405 In the present study, we discuss the potential sensitivity of P-band radar signals, as well as
406 their interpretation for the characterization of soil surface roughness (microtopography and
407 low frequency structures), based on the analysis of backscattering simulations run with an
408 exact numerical model (moment method). Simulations are first considered as a function of
409 microtopography parameters (the $Hrms$ and correlation length) of the soil surface. Roughness
410 parameters typical of agricultural fields are considered in this analysis, which shows that the
411 radar signal increases with $Hrms$ and the correlation length of the soil. A strong correlation is
412 found between the simulated signals and the soil's $Hrms$, with the correlation length having a
413 relatively small influence on the results. To a first approximation, when studying the
414 relationship between simulated radar backscattering and the microtopography of the soil,

415 Hrms can be used alone to represent the terrain's physical structure. Backscattering
416 simulations for a terrain having low frequency structures reveal a combined effect, in which
417 both the rms height, and the structure's correlation length should be taken into account. The
418 MM radar simulations are found to be strongly correlated with the parameter Z_s , with R^2
419 equal to 0.95 at 20°, and 0.98 at 40°. A multi-scale roughness analysis using both roughness
420 scales (H_{rms} , Z_s) reveals the limited influence of small-scale roughness in radar simulations.
421 An empirical roughness spectrum is proposed, based on the use of these two parameters, and
422 is found to be in very good agreement with the previously used analytical (exponential)
423 spectrum. An empirical relationship is proposed to describe the behavior of the backscattered
424 signal as a function of these two parameters. These results illustrate the complexity of
425 interpreting the behavior of P-band radar signals as a function of soil roughness. When the
426 signals simulated with the MM model are compared with real experimental SAR data
427 acquired over various agricultural fields, strong discrepancies are observed, with RMS errors
428 equal to 13.4 dB and 11.2 dB, in the HH and VV polarizations, respectively. These
429 discrepancies could be explained mainly by the absence of an additional roughness scale
430 related to low frequency structures that are not accounted for in local roughness
431 measurements with 2m pinprofiler, with which the MM simulations produce weaker signals.
432 The proposed empirical model can be used to estimate Z_s , lying in the range between 0.3 and
433 3 cm, for the low roughness description of the studied test fields.
434 Despite the usefulness of the parameter Z_s in the description of low frequency structures, it
435 still suffers from some limitations, which should be well understood. This parameter has been
436 introduced in response to the difficulties that are encountered during the inversion of (in
437 general) one or two radar configuration measurements. It must correspond to realistic surface
438 parameters, retrieved from real natural surfaces. As shown by our simulations, under different
439 realistic conditions characterized by approximately the same value of Z_s , we retrieve nearly

440 the same backscattered signal. However, when it is used independently of real data range, or
441 is not used in an inversion process, the same value of Z_s can be retrieved under conditions of
442 extreme roughness leading to different simulations.

443 Backscattering simulations based on numerically generated profiles, making use of different
444 profile lengths (from 1m to 15m) and including the effects of multi-scale roughness, show that
445 the radar simulations become inaccurate when short profile lengths are used. This means that
446 experimental campaigns involving roughness measurements made at the local scale only, for
447 example through the use of a 1m or 2m pin profiler, are inadequate for a complete and
448 accurate analysis of the influence of soil roughness on P-band radar signals. These
449 conclusions are in agreement with studies proposed by Davidson et al., 2000 and Mattia et al.,
450 2001 for higher radar frequencies. When the roughness of low scale structures, determined for
451 example through the use of a fine digital elevation model, is not included in the analysis,
452 significant errors can arise in the estimation of soil roughness and signal strength. This aspect
453 could also concern the retrieval of row orientation, since this parameter is known to have a
454 significant influence at low radar frequencies (Zribi et al., 2002). In the context of the planned
455 BIOMASS space mission, the results presented in the present study highlight the need for
456 further theoretical developments and experimental measurements, in order to improve our
457 understanding of radar-soil interactions in the P band, in particular with respect to the role and
458 characterization of soil roughness as well as the non-negligible effects of volume scattering.

459 **5- Acknowledgments**

460 This study was funded by the TOSCA/CNES project. The authors are grateful to the French
461 Aerospace Research Centre (ONERA) for the acquisition and calibration of the polarimetric
462 RAMSES and SETHI images.

463

464 **6- References**

- 465 Aubert M., Baghdadi N., Zribi M., Ose K., El Hajj M., Vaudour E., and Gonzalez-Sosa E.
466 (2013). Toward an operational bare soil moisture mapping using TerraSAR-X data
467 acquired over agricultural areas, *IEEE Journal of Selected Topics in Applied Earth Observations*
468 *and Remote Sensing*, 6, 2, 900-916.
- 469 Gorrab, A., Zribi, M., Baghdadi, N., Mougenot, B., Lili-Chaabane, Z. (2015). Retrieval of
470 both soil moisture and texture using TerraSAR-X images, *Remote Sensing*, 7, 10098-
471 10116; doi:10.3390/rs70810098.
- 472 Baghdadi N., Paillou P., Davidson M., Grandjean G., and Dubois P. (2000). Relationship
473 between profile length and roughness parameters for natural surfaces. *International*
474 *Journal of Remote Sensing*, 21, 17, 3375-3381.
- 475 Baghdadi, N., King, C., Bourguignon, A., Remond, A. (2002). Potential of ERS and
476 RADARSAT data for surface roughness monitoring over bare agricultural fields:
477 application to catchments in Northern France, *International journal of remote sensing*, 23
478 (17), 3427-3442.
- 479 Baghdadi, N., and Zribi, M. (2006). Evaluation of Radar Backscatter Models IEM, OH and
480 Dubois Using Experimental Observations, *International Journal of Remote Sensing*, 27,
481 18, 3831-3852.
- 482 Baghdadi N., Dubois-Fernandez P., Dupuis X., and Zribi M. (2013). Sensitivity of multi-
483 frequency (X, C, L, P and UHF-band) polarimetric SAR data to soil moisture and surface
484 roughness over bare agricultural soils. *IEEE Geoscience and Remote Sensing Letters*, 10,
485 4, 731-735.
- 486 Blaes, X., Defourny, P. (2008). Characterizing Bidimensional Roughness of Agricultural Soil
487 Surfaces for SAR Modeling , *IEEE Transactions on Geoscience and Remote Sensing*, 46,
488 12, 4050 – 4061.

- 489 Callens, M., Verhoest, N.E.C., Davidson, M.W.J. (2006). Parameterization of tillage-induced
490 single-scale soil roughness from 4-m profiles. *IEEE Transaction on Geoscience and*
491 *Remote Sensing*. 44, 878-888.
- 492 Chen, K. S., Wu, T. D., Tsang, L., Li, Q., Shi, J., and Fung, A. K. (2003). Emission of rough
493 surfaces calculated by the integral equation method with comparison to three-dimensional
494 moment method simulations. *IEEE Transaction on Geoscience and Remote Sensing*, 41
495 (1), 90–101.
- 496 Davidson, M. W. J., Le Toan, T., Mattia, F., Satalino, G., Manninen, T., and Borgeaud, M.
497 (2000) On the characterisation of agricultural soil roughness for radar remote sensing
498 studies, *IEEE Trans. Geosci. Remote Sensing*, 38, 630-640.
- 499 Dubois, P. C., Van Zyl, J., and Engman, T. (1995). Measuring soil moisture with imaging
500 radars. *IEEE Transaction on Geoscience and Remote Sensing*, 33, 915-926.
- 501 Fung, A.K., and Chen, M. F. (1985). Numerical Simulation of Scattering from Simple and
502 Composite Random Surfaces, *J. Opt. Am. A*, 2 (12).²
- 503 Fung, A.K, Li, Z. and Chen, K.S., “Backscattering from a randomly rough dielectric surface,”
504 *IEEE Trans.Geosci. Remote Sensing*, vol. 30, 356-369.
- 505 Fung, A.K., *Microwave Scattering and Emission Models and their Applications*, Norwood:
506 Artech House, 1994.
- 507 Gherboudj I., Magagi R., Berg A. A., and Toth B. (2011) Soil moisture retrieval over
508 agricultural fields from multi-polarized and multi-angular RADARSAT-2 SAR data.
509 *Remote Sensing of Environment*, 115, 1, 33-43.
- 510 Huang, S., Tsang, L., Njoku, E. G., Chen, K. S. (2010) Backscattering coefficients, coherent
511 reflectivities, and emissivities of randomly rough soil surfaces at L-band for SMAP
512 applications based on numerical solutions of Maxwell equations in three-dimensional
513 simulations, *IEEE Transactions on Geoscience and Remote Sensing*, 48, 6, 2557-2568.

- 514 Huang, S., Tsang, L. (2012) Electromagnetic scattering of randomly rough soil surfaces based
515 on numerical solutions of Maxwell equations in three-dimensional simulations Using a
516 hybrid UV/PBTG/SMCG method, *IEEE Transactions on Geoscience and Remote*
517 *Sensing*, 50, 10, 4025-4035.
- 518 Tsang, L., Ding, K. H., Huang, S., Xu, X. (2013) Electromagnetic computation in scattering
519 of electromagnetic waves by random rough surface and dense media in microwave
520 remote sensing of land surfaces, *proceedings of the IEEE*, 101, 2, 255-279.
- 521 Oh, Y., Sarabandi, K., and Ulaby, F. T. (1992). An empirical model and an inversion
522 technique for radar scattering from bare soil surfaces. *IEEE Transactions on Geoscience*
523 *and Remote Sensing*, 30, 370– 381.
- 524 Oh, Y., and Kay, Y.C. (1998). Condition for precise measurement of soil surface roughness,
525 *IEEE Trans. Geosci. Remote Sens.*, 36, 2, 691– 443.
- 526 Le Toan T., S. Quegan, M. Davidson, H. Balzter, P. Paillou , K. Papathanassiou, S. Plummer,
527 S. Saatchi, H. Shugart, L. Ulander. (2011). The BIOMASS Mission : Mapping global
528 forest biomass to better understand the terrestrial carbon cycle, *Remote Sensing of*
529 *Environment*, 115, 2850-2860.
- 530 Le Morvan, A., Zribi, M., Baghdadi, N., and Chanzy, A. (2008). Soil moisture profile effect
531 on radar signal measurement, *Sensors*, 8, 256-270.
- 532 Lievens, H., Vernieuwe, H., Alvarez-Mozos, J., de Baets, B., Verhoest, N.E.C. (2009). Error
533 in SAR-derived soil moisture due to roughness parameterization: An analysis based on
534 synthetical surface profiles. *Sensors*, 9, 1067–1093.
- 535 Mattia, F., Le Toan, T., Davidson, D. (2001). An analytical, numerical, and experimental
536 study of backscattering from multiscale soil surfaces, *Radio Science*, 36, 119–135.
- 537
538
539 .

- 540 Paloscia, S., Pampaloni, P., Pettinato, S., Santi, E. (2010). Generation of soil moisture maps
541 from ENVISAT/ASAR images in mountainous areas: a case study, *International Journal*
542 *of Remote Sensing*, 31(9), 2265 - 2276.
- 543 Peplinski, N.R., Ulaby, F.T., and Dobson, M.C. (1995). Dielectric Properties of Soils in the
544 0.3-1.3-GHz Range, *IEEE Transactions on Geoscience and Remote Sensing*, Vol. 33, No.
545 3, 803-807.
- 546 Peplinski, N.R., Ulaby, F.T., and Dobson, M.C. (1995). Corrections to Dielectric Properties of
547 Soils in the 0.3-1.3-GHz Range, *IEEE Transactions on Geoscience and Remote Sensing*,
548 Vol. 33, No. 6, 1340.
- 549 Pierdicca, N., Pulvirenti, L., Bignami, C. (2010). Soil moisture estimation over vegetated
550 terrains using multitemporal remote sensing data, *Remote Sensing of environment*, 114,
551 2, 440-448
- 552 Rahman, M.M., Moran, M.S., Thoma, D.P., Bryant, R., Holifield Collins, C.D., Jackson, T.,
553 Orr, B.J., Tischler, M. (2008). Mapping surface roughness and soil moisture using multi-
554 angle radar imagery without ancillary data, *Remote sensing of environment*, 112, no. 2,
555 391-402.
- 556 Rakotoarivony, L., Taconet, O., Vidal-madjar, D., Bellemain, P. and Benalle`gue, M., 1996,
557 Radar backscattering over agricultural bare soils. *Journal of Electromagnetic Waves and*
558 *Applications*, 10, pp. 187- 209.
- 559 Shi, J., Wang, J., Hsu, A. Y., O'Neill, P. E., & Engmann, T. (1997). Estimation of bare
560 surface soil moisture and surface roughness parameter using L-band SAR image data.
561 *IEEE Transactions on Geoscience and Remote Sensing*, 35, 1254–1265.
- 562 Ulaby, F.T., Kouyate, F., Fung, A.K., Sieber, A.J. (1982), A Backscatter Model for a
563 Randomly Perturbed Periodic Surface , *IEEE Transactions on Geoscience and Remote*
564 *Sensing*, Volume: GE-20, Issue: 4, 518 - 528.

- 565 Ulaby, F.T., Moore, R.K., and Fung, A.K., *Microwave Remote Sensing Active and Passive*.
566 Norwood: Artech House, inc, 1986.
- 567 Verhoest, N. E. C., Lievens, H., Wagner, W., Alvarez-Mozos, J., Moran, M. S., and Mattia, F.
568 (2008). On the soil roughness parameterization problem in soil moisture retrieval of bare
569 surfaces from Synthetic Aperture Radar. *Sensors*, 8 (7), 4213–4248.
- 570 Zribi, M., Taconet, O., Le Hégarat-Masclé, S., Vidal-Madjar, D., Emblanch, C., Loumagne,
571 C., and Normand, M. (1997). Backscattering behavior and simulation comparison over
572 bare soils using SIRC/XSAR and ERASME 1994 data over Orgeval, *Remote Sens.*
573 *Environ*, 59, 256-266.
- 574 Zribi, M., Ciarletti, V., Taconet, O., and Vidal-Madjar, D. (2002). Effect of rows structure on
575 radar microwave measurements over soil surface, *International Journal of Remote*
576 *Sensing*, 23, 24, 5211-5224.
- 577 Zribi, M., and Dechambre, M. (2003). An new empirical model to retrieve soil moisture and
578 roughness from Radar Data. *Remote Sens. Environ*, 84, 42-52.
- 579 Zribi, M., Baghdadi, N., Holah, N., Fafin, O., and Guérin, C. (2005). Evaluation of a rough
580 soil surface description with ASAR-ENVISAT Radar Data. *Remote sensing of*
581 *environment*, 95, 67-76.
- 582 Zribi, M., Baghdadi, N. and Guérin, C. 2006, Analysis of surface roughness heterogeneity and
583 scattering behaviour for radar measurements, *IEEE Transactions on Geoscience and*
584 *Remote Sensing*, 44, 9, 2438-2444.
- 585 Zribi, M., Chahbi, A., Lili Chabaane, Z., Duchemin, B., Baghdadi, N., Amri, R., Chehbouni,
586 A.. (2011). A. Soil surface moisture estimation over a semi-arid region using ENVISAT
587 ASAR radar data for soil evaporation evaluation. *Hydrol. Earth Syst. Sci.*15, 345–358.
588

589 Zribi, M., Gorrab, A., Baghdadi, N. (2014a). A new soil roughness parameter for the
590 modelling of radar backscattering over bare soil. *Remote Sens. Environ.* 152, 62–73.

591 **Zribi, M., Gorrab, A.,** Baghdadi, N., Lili-Chabaane, Z., Mougenot, B. (2014b). Influence of
592 radar frequency on the relationship between bare surface soil moisture vertical profile
593 and radar backscatter, *IEEE Geoscience and Remote Sensing Letters*, 11(4)
594 848 - 852.

595 Zribi, M., Sahnoun, M., Dusséaux, R., Afifi, S., Baghdadi, N., Ben Hamida, A. (2016).
596 Analysis of P band radar signal potential to retrieve soil moisture profile, ATSSIP'2016,
597 Monastir, Tunisia, 21-24 March, 2016.

598

599 Figures and tables

600

601 Table 1: Empirical values of the roughness parameters a_θ , b_θ , c_θ and d_θ

602 Table 2: Values of the empirical model parameters, for incidence angles equal to 20° and 40° ,
603 in the HH polarization.

604 Table 3: Characteristics of the ground truth measurements. θ : Incidence angle, m_v :
605 Volumetric soil moisture (0-10 cm), $Hrms$: Root mean square surface height, l : Correlation
606 length.

607 Figure 1: Backscattering simulations as a function of surface roughness, corresponding in the
608 case of (a) and (b) to: microtopography ($Hrms$) with correlation lengths l equal to 4, 6, 8 and
609 10 cm, and in the case of (c) and (d) to: a low spatial frequency rms height (Sg), with
610 correlation lengths Lg equal to 40, 60, 80 and 100 cm. All simulations are made in the HH
611 polarization with a soil moisture value of $20 \text{ cm}^3/\text{cm}^3$. The simulations in (a) and (c) are made
612 at a 20° incidence angle, and those of (b) and (d) are made at a 40° incidence angle.

613 Figure 2: Exponential roughness spectrum as a function of wave number

614 Figure 3: Backscattering simulations in the HH polarization, as a function of the parameter Zs
615 (cm): Sg lies in the range between 4 and 10 cm, Lg between 40 and 100 cm, $m_v = 20$
616 cm^3/cm^3 , a) 20° incidence angle, b) 40° incidence angle.

617 Figure 4: Synthetically generated surface profiles: micro-topography ($Hrms=0.6\text{cm}$, $l=6\text{cm}$)
618 and multi-scale roughness ($Hrms=0.6\text{cm}$, $l=6\text{cm}$, $Sg=6\text{cm}$, $Lg=100\text{cm}$).

619 Figure 5: MM backscattering simulations (in decibels) as a function of the two roughness
620 parameters ($K.Hrms$, $K.Zs$), a) 20° incidence angle, b) 40° incidence angle.

621 Figure 6: Intercomparison between roughness spectrum values retrieved with exponential
622 spectrum and empirical relationship (6), for all roughness conditions considered for MM
623 simulations ($Hrms$ ranged between 0.4 cm and 2 cm, l ranged between 4 and 10cm, Sg ranged

624 between 4 and 14cm and L_g ranged between 40 and 100cm), at incidence angle equal to: a)
625 20° incidence angle, b) 40° incidence angle.

626 Figure 7: Comparison of radar backscattering predicted by the empirical model defined in
627 equation (7), with the results predicted by MM simulations using the same set of roughness
628 conditions as for the simulations shown in Fig. 5, at incidence angles equal to a) 20° , b) 40° .

629 Figure 8: Location of two study sites in France (Bordeaux and Garons).

630 Figure 9: Simulated MM radar signals as a function of measured radar signals over
631 agricultural fields, a) HH pol (b) VV pol.

632 Figure 10: Estimated values of Z_s , plotted as a function of the in situ values of H_{rms}
633 measured on eight test fields.

634 Figure 11: Variations in simulated radar signal as a function of the length of the soil profiles,
635 including the effects of multiscale roughness ($H_{rms}=0.6\text{cm}$, $l=6\text{cm}$, $S_g=6\text{cm}$, $L_g=100\text{cm}$).